cigre Turkey

TEPES
TURKISH JOURNAL OF ELECTRICAL POWER AND ENERGY SYSTEMS

TEPES, 2023 [epub ahead of print] **DOI:** 10.5152/tepes.2023.23003

RESEARCH ARTICLE

# Analysis of Photovoltaic System in Unbalanced Distribution Systems Considering Ambient Temperature and Inverter Efficiency

**Salman Ahmed Nur, Selçuk Emiroğlu**

Department of Electrical and Electronics Engineering, Sakarya University, Sakarya, Turkey

**Cite this article as:** S. A. Nur and S. Emiroğlu, "Analysis of photovoltaic system in unbalanced distribution systems considering ambient temperature and inverter efficiency," *Turk J Electr Power Energy Syst.*, 2023, [epub ahead of print].

## ABSTRACT

This paper investigates the impacts of solar irradiance, ambient temperature, and solar inverter efficiency on the performance of a photovoltaic system. The analysis of the system has been performed on the unbalanced IEEE 13-node test feeder. The loads connected to the feeder are modeled as constant impedance, constant current, constant power (ZIP) loads, and the daily load profiles of three customers (commercial, industrial, and residential) are employed. A daily power flow simulation at 1-minute intervals has been carried out using Open Distribution System Simulator (OpenDSS). The PV system performance has been evaluated using numerical simulations under three weather conditions, namely sunny, semi-cloudy, and overcast. The results show that the PV system generates more power on sunny and semi-cloudy days while the PV output power is very low on an overcast day due to the extremely low solar irradiance. In addition, the energy demand from the substation and the power loss has been reduced with the deployment of the photovoltaic system into the distribution system. Moreover, when the ambient temperature and inverter efficiency are considered, the PV system produced more power in sunny and overcast conditions compared to when these factors are not taken into consideration or assumed the temperature is constant throughout the day. This result shows the effect of the temperature of the selected region on the performance of the PV system. The losses due to the inverter and temperature can be reduced by appropriately sizing the inverter and choosing a proper location with high solar irradiance and low temperature, respectively.

**Index Terms—**Ambient temperature, inverter efficiency, photovoltaic, power loss, unbalanced distribution systems

## I. INTRODUCTION

The impacts of climate change have been increasingly witnessed all over the world. Rising temperatures and drought frequency are affecting millions of people around the world. Regarding this, renewable energy sources such as solar are increasingly being used to meet energy needs and are seen as potential solutions to tackle serious energy crises and environmental concerns [1]. One of the most abundant renewable resources is solar energy, which is projected to be the fundamental basis for a sustainable energy economy. The power produced by a photovoltaic (PV) cell relies on several factors and these are categorized in [2] as follows: PV system, cost, installation, environmental, and miscellaneous factors. Several environmental factors such as shadows, dust, temperature, and solar radiation impact the PV system's output power. A significant factor of uncertainty that can complicate energy planning and jeopardize investment opportunities in the power industry is the vulnerability of PV systems to future climate patterns. The impacts of extreme weather and climatic conditions on PV power outputs have been studied in [3]. Higher temperatures and persistent cloud cover reduce the output power of the PV system. Power electronics are also a crucial part of PV production. Several power converter topologies and power tracking methods have been proposed in [4]. The efficiency of PV inverters has increased over time and achieved values over 97% [5]. The thermal behavior of PV systems has been studied recently in [6, 7]. The open circuit voltage is significantly impacted by the rise in cell temperature; it decreases linearly with rising cell temperature. The PV output power relies on solar insolation that can fluctuate significantly as clouds pass overhead. Unless appropriate measures are taken, this can result in significant negative power quality at high-level penetrations [8]. Historically, the distribution system was planned based on peak demand. With the proliferation of distributed resources such as PV, it has become crucial for grid planners to analyze and design for dynamic conditions [9]. Therefore, it is essential to accurately predict PV power output under real weather conditions. The impact of voltage fluctuations due to the moving cloud shadows on the distribution system with high PV penetration is assessed in [10]. The impact of temperature and irradiance on key parameters of various PV cell types was investigated in [11]. Furthermore, several studies on the impact of PV penetration on

**Corresponding author:** Salman Ahmed Nur, salmaanahmednuur@gmail.com

**Received:** January 8, 2023
**Accepted:** March 6, 2023
**Publication Date:** May 15, 2023

the distribution network have been carried out. Mohanty et al. investigated the impact of PV penetration on an unbalanced distribution network with dynamic load conditions [12]. Results reveal that loss occurs comparatively less in buses with capacitors and more in buses without capacitors. Additionally, the voltage profile remained within the desired range and the PV injection has not resulted in an abrupt increase or decrease in bus voltages. Moreover, Radatz et al. assessed various distributed generation penetration levels in a real distribution feeder [9]. These studies, however, have not examined the impact of PV systems on distribution networks when ambient temperature and inverter efficiency are taken into account. This is why this study has been carried out. The contribution of this paper is to analyze the impact of PV systems on distribution networks considering the temperature and inverter efficiency using three load profiles and three solar irradiance data with 1-minute resolution.

In this paper, an accurate simulation of the effect of PV on the distribution network is investigated by considering temperature, solar irradiance, and inverter efficiency parameters. For that purpose, a 1-minute step size simulation is carried out on Institute of Electrical and Electronics Engineers (IEEE) 13-node system using Open Distribution System Simulator (OpenDSS) [13]. Three weather conditions which are sunny, semi-cloudy, and overcast have been used to analyze the PV system. Moreover, the analysis of the PV system has been conducted by considering ambient temperature and inverter efficiency as these affect the output of the PV system. Then, the effect of ambient temperature and inverter efficiency on the PV system's output has also been demonstrated by comparing it with the PV system case which considers only the solar irradiance. Following this introductory part, the distribution network and the voltage-dependent load model (ZIP) used in this study are explained in Section II. In section III, the study location and the data of irradiance, temperature, and inverter efficiency, as well as the modeling of the PV array and the inverter element in OpenDSS are presented. Finally, case studies and simulation results are presented in Section IV and the conclusion is given in Section V.

## II. DISTRIBUTION NETWORK DESIGN

### A. IEEE 13-Node Radial Distribution Feeder

The IEEE 13-node test feeder has been used in this study to evaluate the PV system's impact on an unbalanced distribution system. The IEEE 13-node test feeder is characterized by the type of load (spot and distributed loads), line types (single-/three-phase overhead and underground lines), voltage regulators, shunt capacitors, and transformers. The voltage regulator operates based on line drop compensation. The data about the system are explained in [14]. This system has total active and reactive power loads of 3466 kW and 2102 kVAr, respectively. The single-line diagram for the modified test feeder is represented in Fig. 1.

**Main Points**

- The effect of solar irradiance, ambient temperature, and inverter efficiency on the photovoltaic (PV) system in unbalanced distribution systems has been investigated by using OpenDSS.
- A daily power flow simulation with a 1-minute step size has been performed to evaluate the effect of short-term PV fluctuation on the distribution system.
- Three irradiance curves representing sunny, semi-cloudy, and overcast weather conditions have been considered.
- Three case studies have been conducted to assess the impact of PV integration into the distribution network.
- By integrating PV into the network, the power loss and the power drawn by the substation have been reduced.

### B. Load Modeling

Two main approaches have been traditionally used to develop load models: the component-based approach and the measured-based approach [15]. The component-based approach relies on knowledge of the individual components that make up the load while the measured-based approach is based on how the load behaves when subjected to voltage variations [15]. The load selection criteria depend on the type of analysis performed and the load's characteristics. In the steady state power flow studies, loads can be modeled as static. One of the most common static load models is the second-order polynomial load model, composed of constant impedance, current, and power characteristics. The static model is also known as the ZIP model [16].

Table I shows the ZIP coefficients [17] for commercial, residential, and industrial customer classes and the nodes at which the loads are connected. The active and reactive power of the ZIP coefficients model is given in (1) and (2).

$$P = P_0\left[Z_p\left(\frac{V}{V_0}\right)^2 + I_P\frac{V}{V_0} + P_P\right] \quad (1)$$

$$Q = Q_0\left[Z_q\left(\frac{V}{V_0}\right)^2 + I_q\frac{V}{V_0} + P_q\right] \quad (2)$$

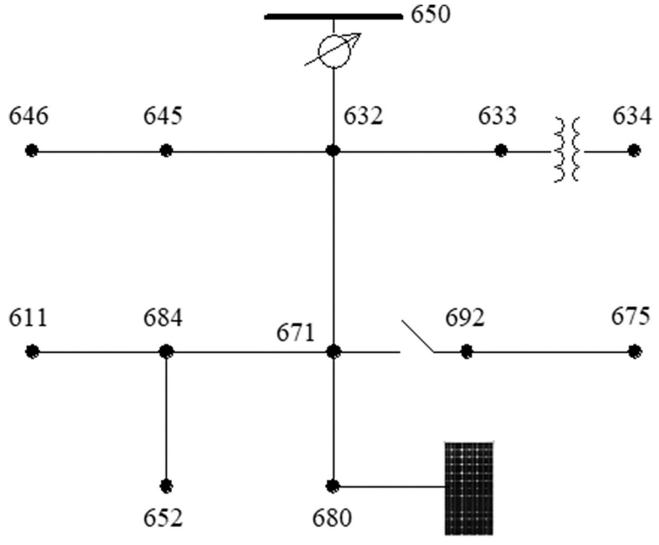


**Fig. 1.** The modified IEEE 13-node test feeder [13].

**TABLE I.**
ZIP COEFFICIENTS AND THE NODES OF DIFFERENT LOAD TYPES [4]

| Class | $Z_p$ | $I_p$ | $P_p$ | $Z_q$ | $I_q$ | $P_q$ | Load Nodes |
|---|---|---|---|---|---|---|---|
| Residential | 0.85 | −1.12 | 1.27 | 10.96 | −18.73 | 8.77 | 671-634-652-611 |
| Commercial | 0.43 | −0.06 | 0.63 | 4.06 | −6.65 | 3.59 | 692-645-646 |
| Industrial | 0 | 0 | 1 | 0 | 0 | 1 | 670-675 |

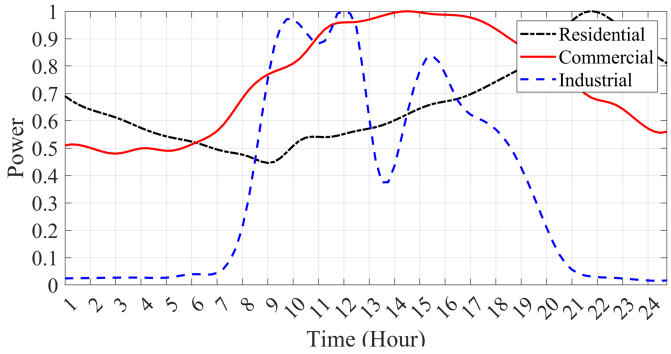


**Fig. 2.** Load shapes for different customers [17].

The load shapes presented in Fig. 2 show 24-hour normalized load shapes for residential, commercial, and industrial customers and are taken from [17]. One can deduce that the peak power demand varies depending on the type of customers.

## III. PHOTOVOLTAIC SYSTEM MODELING

The model of the PV system in OpenDSS is a combination of the PV array and the PV inverter which is useful for distribution system studies [18]. The block diagram of the model has been depicted in Fig. 3.

### A. Irradiation Curves and Temperature

The output power of PV plants is intermittent and heavily relies on the weather condition and the time of day. Days with clouds or rain cause significant fluctuations in PV power output [19]. In this study, the impact of three solar irradiances on the output of PV production has been analyzed. The datasets used have been retrieved from a network composed of 24 irradiance sensors measuring solar irradiance (global horizontal irradiance, W/m$^2$) in Alderville (Ontario) [20]. These datasets correspond to three categories: clear-sky(sunny), overcast, and variable(semi-cloudy) days. The solar irradiance has been measured on 2015-03-24 for clear sky, 2015-02-08 for overcast, and 2015-10-08 for semi-cloudy. Each dataset is defined as a 1-minute step size for 24-hour period making a total of 1440 data. The selected location for the study has a latitude of 44.190159 (°) and a longitude of −78.096701(°). The three irradiation curves are shown in Fig. 4.

Three temperature data for sunny, semi-cloudy, and overcast conditions have been obtained in this study. The data consist of 1-minute intervals for 24 hours corresponding to the same days of the

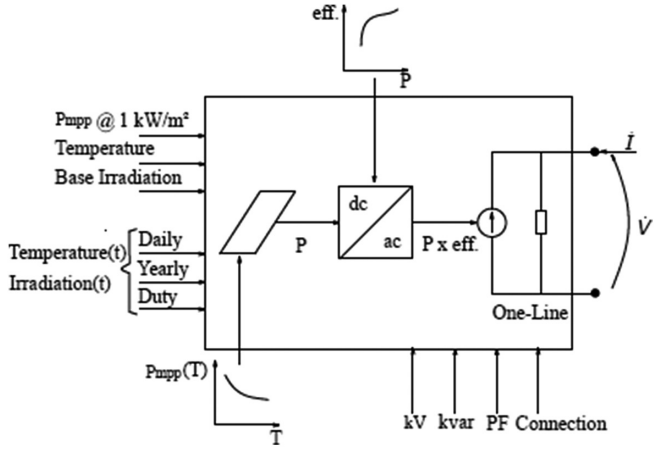


**Fig. 3.** Photovoltaic system model in OpenDSS [9].

previously mentioned solar irradiance data has been. The temperature data were originally obtained as ambient temperature (Fig. 5) from the National Aeronautics and Space Administration (NASA) Langley Research Center Prediction of Worldwide Energy Resource Project funded through the NASA Earth Science/Applied Science Program [21]. However, in OpenDSS, the PV element model

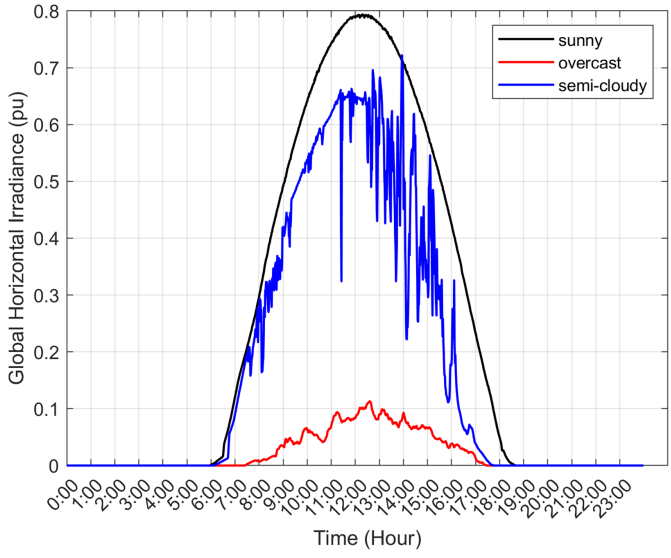


**Fig. 4.** Irradiation curves for sunny, semi-cloudy, and overcast days.

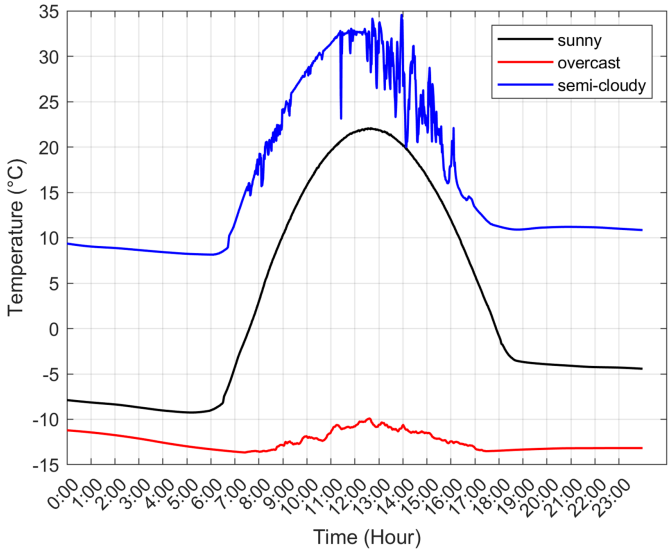


**Fig. 5.** Ambient temperature for sunny, semi-cloudy, and overcast days.

uses panel temperature ($T_c$). Therefore, the $T_c$ has been calculated using (3) presented in [22]. The wind effect is not considered in the equation.

$$T_c = T_a + \left(\frac{T_{NOCT} - T_{a,NOCT}}{G_{NOCT}}\right) G_T \tag{3}$$

where the $T_c$ is the cell temperature, $T_a$ is the ambient temperature, $T_{NOCT}$ is the nominal operating cell temperature (NOCT) (43°C was taken in this study ), $T_{a,NOCT}$ is the ambient temperature considered for NOCT conditions (20°C), $G_T$ is the plane module irradiance, and $G_{NOCT}$ is the solar irradiance for NOCT condition (800 W/m$^2$). The PV panel temperature at the selected location with the ambient temperature given in Fig. 5 is shown in Fig. 6.

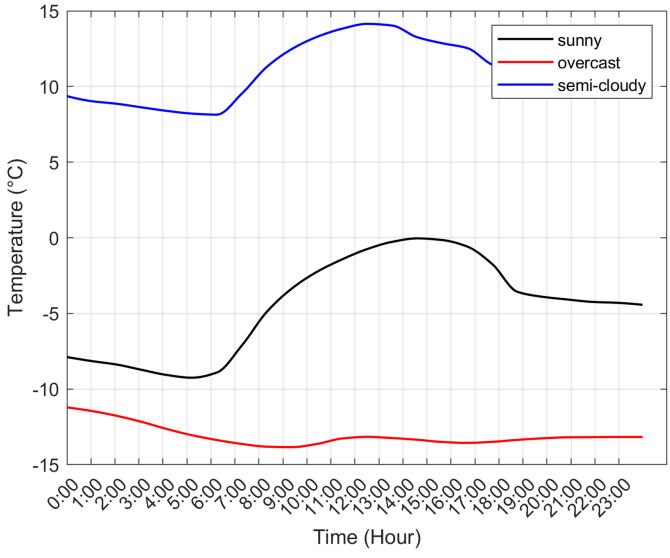


**Fig. 6.** Panel temperature for sunny, semi-cloudy, and overcast days.

### B. Photovoltaic Array

The PV element is connected to node 680 of the IEEE 13-node test feeder as shown in Fig. 1. In OpenDSS, for the model to calculate the output power of the PV array (*panelKW*), it requires the data of irradiance, temperature (*T*) factor, and rated power of the panel at the maximum power point ($P_{mpp}$) defined at 1 kW/m$^2$ irradiance and a constant panel temperature (25°C) [18]. The $P_{mpp}$ of the PV array has been chosen to be 1000 kW with a power factor of 1. The maximum power output of the panel is calculated using (4).

$$P(panelKW) = P_{mpp} \times irradience \times factor(@\,actualT) \tag{4}$$

The temperature coefficient affects the power output of PV panels and the power output of the PV decreases linearly as the temperature increases. The panel output is then reduced by a factor based on the temperature of the panel. The power versus temperature curve shown in Fig. 7 is defined using (5). The power decreases by about 18% as the panel temperature rises from 25°C to 85°C. In this study, the manufacturer datasheet of the AS-MQ7-156 HC solar PV module has been used. The temperature coefficient from the datasheet has been taken into account to calculate the maximum power produced by the PV at various irradiances and temperatures using the equation given in (5) [12].

$$P_{\max} = P_{\max(STC)} \frac{G}{1000}\left[1 + TC\left(P_{\max}, G\right)\left(T_C - 25\right)\right] \tag{5}$$

where $P_{max(STC)}$ is the maximum power of the photovoltaic cell at Standard Test Condition (600 W), $G$ is the solar irradiance (1000 W/m$^2$), $T_C$ is the temperature of the photovoltaic cells, and $TC$ ($P_{max}$, $G$) is the temperature coefficient for the at irradiance G (–0.36%/°C). The relationship of the $P_{mpp}$–temperature curve for a PV panel rated power in 1 pu at 25°C is shown in Fig. 7.

### C. Inverter Efficiency Curve and Optimum Inverter Sizing

The DC power produced by the PV panel must be converted to AC power by solar inverters to be injected into the grid. In this work, a mathematical method presented in [23] has been used to determine the optimum inverter size. The equation for selecting the optimum inverter output power is presented in (6):

$$P_{inv,N}^{opt} = P_{max}\sqrt{\frac{B}{3C}} \tag{6}$$

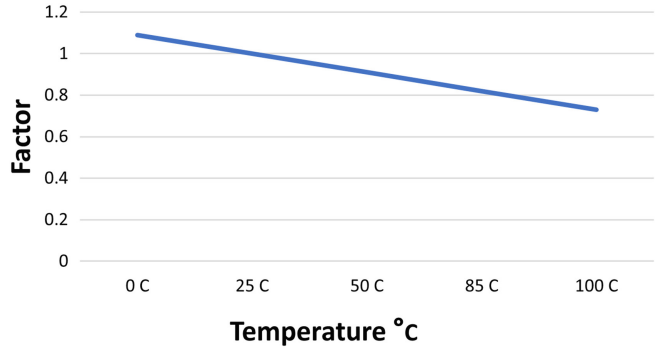


**Fig. 7.** Power–temperature factor for 1 kW/m$^2$ irradiance.

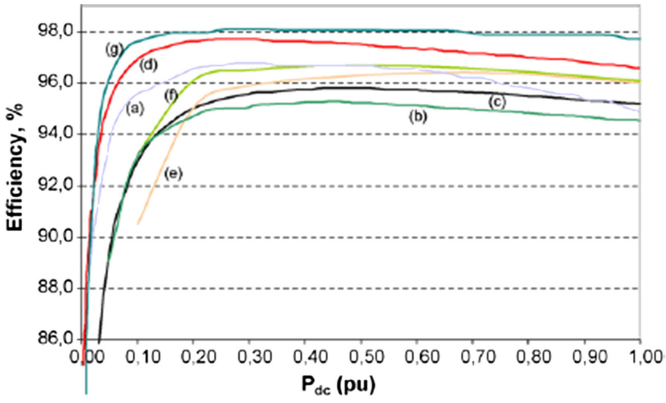


**Fig. 8.** The efficiency curves of different solar inverters. (a) Solar Konzept, 2 kW; (b) Sunways, 3.6 kW; (c) SMA, 5 kW; (d) SMA, 11 kW; (e) Satcon, 50 kW; (f) Satcon, 100 kW; (g) Siemens, 1000 kVA [22].

**TABLE II.**
CASE SCENARIOS

| Case | Scenario | Connection | |
|---|---|---|---|
| | | Generator | PV |
| BASECASE | | × | × |
| GENCASE | Sunny | ✓ | × |
| | Cloudy | ✓ | × |
| | Overcast | ✓ | × |
| PVCASE | Sunny | × | ✓ |
| | Cloudy | × | ✓ |
| | Overcast | × | ✓ |

✓ stands for: there is a connection.
× stands for: there is no connection.

where *B* and *C* parameters are determined from the efficiency curves of the inverter shown in Fig. 8, and the $P_{max}$ is the highest produced power from the panel. In this work, the maximum DC power output of the PV is 785 kW. As a result, an optimal size of 1330 kVA rated inverter has been selected using the *B* and *C* parameters of Siemens 1000 kVA inverter presented in [23]. In OpenDSS, the inverter model finds the *mpp* within the simulation time step. The efficiency curve of various inverters is shown in Fig. 8.

## IV. RESULTS

In this work, the daily mode simulation has been performed using the OpenDSS software [13]. This mode calculates the power flow for a period of 24 hours. A total number of 1440 power flow simulations have been performed considering a 1-minute interval. Three cases are designed to evaluate the impact of PV penetration into the grid: the BASECASE, the GENCASE, and the PVCASE. Both GENCASE and PVCASE have three scenarios namely; sunny, semi-cloudy, and overcast. The case scenarios are summarized in Table II.

The BASECASE is the case in which the simulation is conducted on the original IEEE 13-node test system with no PV. The results of this case are then recorded to compare with the other two cases. In the second case (GENCASE), a 1000 kW generator is connected to node 680 to evaluate the distribution network. The generator element in OpenDSS can be modeled with the consideration of daily solar irradiation without the temperature effect. In this case, it is assumed that the generator behaves as a PV system without considering the effect of the temperature variation (assuming it is constant at 25°C during the day) and the inverter efficiency. Therefore, three daily irradiance curves (sunny, semi-cloudy, and overcast) are used to model the generator. Case 3 is the PVCASE in which the PV is connected to node 680. In this case, the inverter efficiency and the panel temperature are taken into account to assess the impact of the PV system on the distribution systems. The three irradiance and temperature curves are used to model the PV element.

Table III compares the daily simulation results obtained from the BASECASE and the three GENCASE scenarios (sunny, semi-cloudy, and overcast). The total energy generated is equal to the sum of the energy consumed by the load and the energy loss in both cases, as illustrated in the table. For GENCASE, the generated power at node 680 is the highest during the GENCASE(sunny) at 5859 kWh followed by the GENCASE(semi-cloudy) and GENCASE(overcast) at 4155 kWh and 531 kWh, respectively. The energy losses of the feeder and substation demand have also been reduced for the three GENCASE scenarios when compared to the BASECASE. The greatest energy loss reduction is 19.44% for GENCASE(sunny), followed by 14.31% and 2.01% for GENCASE(semi-cloudy) and GENCASE(overcast), respectively. Figs. 9, 10, 11 and 12 show the daily active power flowing through the substation for BASECASE and GENCASE scenarios.

**TABLE III.**
COMPARISON BETWEEN BASECASE AND GENCASE

| Various Cases | Energy Measured at Substation (kWh) | Energy Measured at Node 680 (kWh) | Energy Consumed by the Loads (kWh) | Energy Losses of the Network (kWh) | Energy Loss Reduction (%) |
|---|---|---|---|---|---|
| BASECASE | 52 664 | - | 51 574 | 1090 | |
| GENCASE(sunny) | 46 570 | 5859 | 51 551 | 878 | 19.44% |
| GENCASE(semi-cloudy) | 48 378 | 4155 | 51 599 | 934 | 14.31% |
| GENCASE(overcast) | 52 117 | 531 | 51 580 | 1068 | 2.01% |

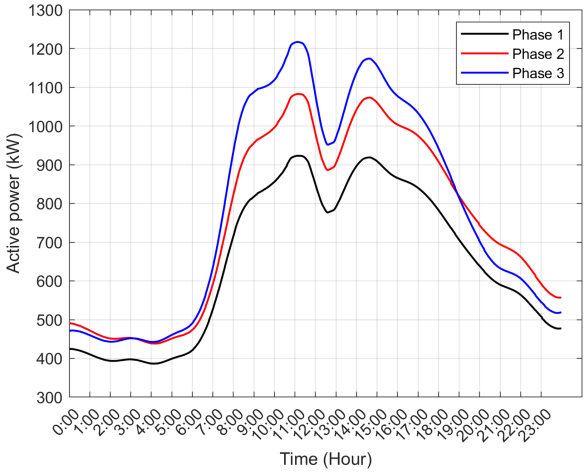


**Fig. 9.** Power in each phase at the substation for BASECASE.

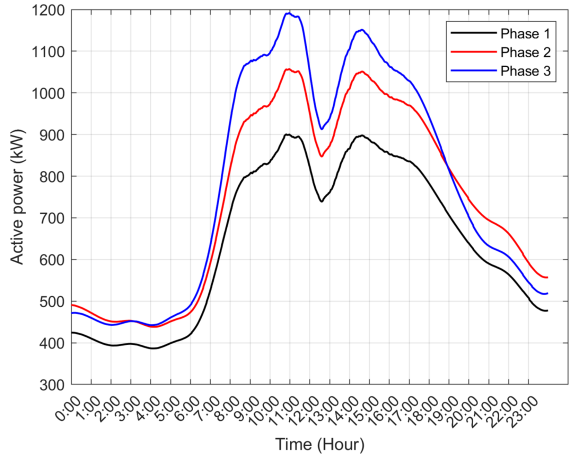


**Fig. 12.** Power in each phase at the substation for GENCASE (overcast).

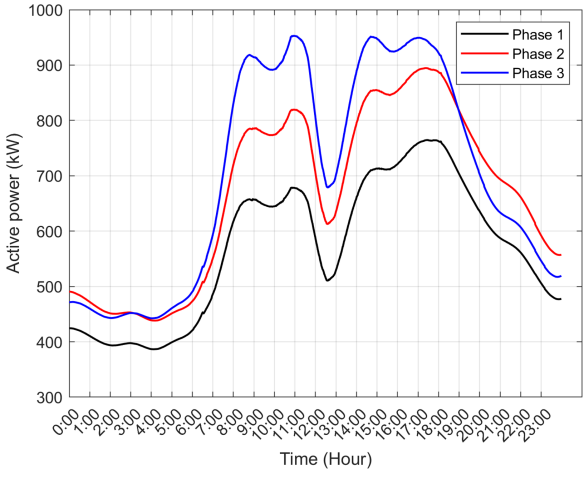


**Fig. 10.** Power in each phase at the substation for GENCASE (sunny).

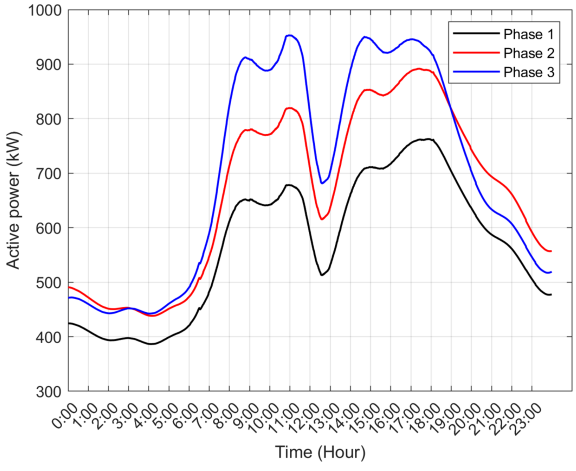


**Fig. 13.** Power in each phase at the substation for PVCASE (sunny).

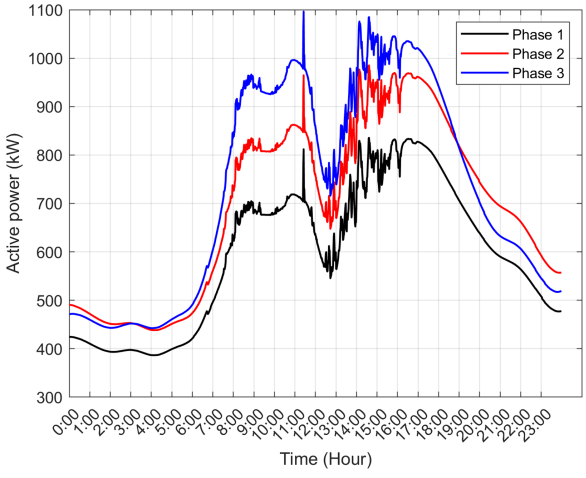


**Fig. 11.** Power in each phase at the substation for GENCASE (semi-cloudy).

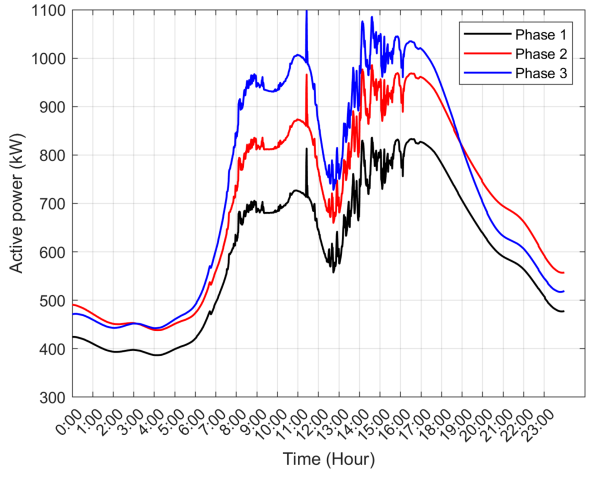


**Fig. 14.** Power in each phase at the substation for PVCASE (semi-cloudy).

**TABLE IV.**
COMPARISON BETWEEN BASECASE AND PVCASE

| CASE | Energy Measured at Substation (kWh) | Energy Measured at Node 680 | Energy Consumed by the Loads (kWh) | Energy Losses (kWh) | Loss Reduction |
|---|---|---|---|---|---|
| BASECASE | 52 664 | - | 51 574 | 1090 | |
| PVCASE(sunny) | 46 501 | 5926 | 51 552 | 875 | 19.72% |
| PVCASE(semi-cloudy) | 48 500 | 4037 | 51 599 | 938 | 13.94% |
| PVCASE(overcast) | 52 059 | 587 | 51 580 | 1066 | 2.2% |

The total energy generated, energy consumed, and energy losses for BASECASE and PVCASE are presented in Table IV. The energy demand from the substation and the energy losses of the network have been reduced for all the PVCASE scenarios. The highest energy loss reduction is achieved in PVCASE(sunny) at 19.72% compared to the PVCASE(semi-cloudy) at 13.94% and PVCASE(overcast) at 2.2%. The daily active power flow through the substation for PVCASE is given in Figs. 13, 14 and 15.

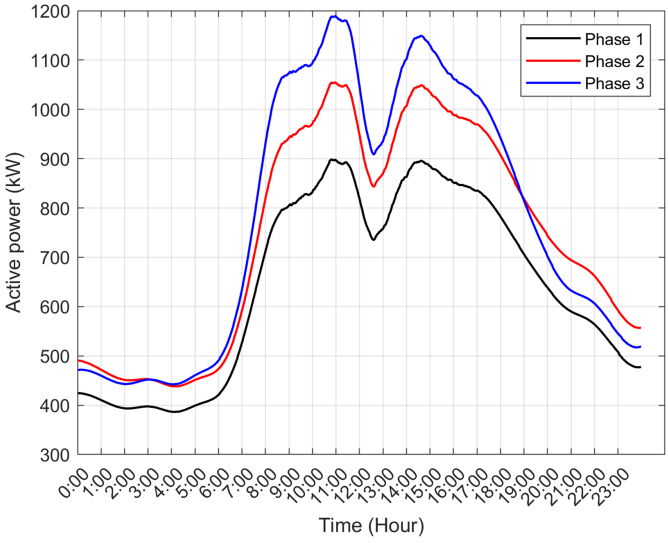


**Fig. 15.** Power in each phase at the substation for PVGENCASE (overcast).

**TABLE V.**
COMPARISON BETWEEN PVCASE AND GENCASE

| Scenario | Daily PV Panel Energy Output (kWh) | Energy Measured at Node 680 for PVCASE (kWh) | Energy Measured at Node 680 for GENCASE (kWh) | Energy Difference Between PV Output and PVCASE (kWh) |
|---|---|---|---|---|
| Sunny | 6044 | 5926 | 5859 | 118 |
| Semi-cloudy | 4118 | 4037 | 4155 | 81 |
| Overcast | 600 | 587 | 531 | 13 |

The comparison between the energy measured in PVCASE, GENCASE, and PV panel output is presented in Table V. When the effect of inverter efficiency and temperature is not taken into account in GENCASE, the energy measured is 5859 kWh for sunny, 4155 kWh for semi-cloudy, and 531 kWh for overcast. When the temperature effect alone is considered, the energy measured at the PV output has increased for sunny and overcast conditions by 3.06% and 11.5%, respectively, compared to GENCASE. However, for semi-cloudy weather, the PV energy output has decreased by 0.9%. This is because the temperature in the selected region is below 25°C on sunny and overcast days, but above 25°C on semi-cloudy days. This result shows the impact of temperature on PV power output.

The difference between the energy output of the PV and the energy measured at node 680 for PVCASE is 118 kWh for sunny weather, 81 kWh for cloudy weather, and 13 kWh for overcast weather. These energy differences are due to the inverter loss. Because the inverter used in the study has high efficiency (see Section III), the energy losses caused by the inverter are relatively low. These losses would have been greater if a lower efficiency inverter had been chosen. This result emphasizes the significance of selecting an appropriate inverter.

## V. CONCLUSION

This paper assesses the impact of a PV system on unbalanced distribution power systems considering temperature, irradiance, and inverter efficiency. The study has been tested on the IEEE 13-node test feeder with a ZIP load model and different customer types using OpenDSS. The daily simulation mode has been conducted on three different case scenarios. The results indicate that when the effect of temperature alone is considered, the PV panel produced more energy by 3.06%, and 11.5% for PVCASE (sunny) and PVCASE (overcast), respectively, compared to GENCASE scenarios. However, when the impact of both the inverter and temperature is taken into account, the injected power to the grid has decreased to 1.95% and 2.16% for PVCASE (sunny) and PVCASE (overcast), respectively. By connecting the PV to the network, energy losses and energy demand from the substation are reduced. Moreover, it has been observed that the efficiency of the selected inverter and the ambient temperature affect the amount of power injected by the PV system. Therefore, it is concluded that the weather conditions of the PV site and the inverter selection should be considered during PV system integration into the distribution systems.

**Peer-review:** Externally peer-reviewed.

**Declaration of Interests:** The authors have no conflicts of interest to declare.

**Funding:** The authors declared that this study has received no financial support.

## REFERENCES

1. IRENA, *Renewable Energy Targets in 2022: A Guide to Design*. Abu Dhabi: International Renewable Energy Agency, 2022.
2. M. M. Fouad, L. A. Shihata, and E. I. Morgan, "An integrated review of factors influencing the performance of photovoltaic panels," *Renew. Sustain. Energy Rev.*, vol. 80, pp. 1499–1511, 2017. [CrossRef]
3. S. Feron, R. R. Cordero, A. Damiani, and R. B. Jackson, "Climate change extremes and photovoltaic power output," *Nat. Sustain.*, vol. 4, no. 3, pp. 270–276, 2021. [CrossRef]
4. A. Bughneda, M. Salem, A. Richelli, D. Ishak, and S. Alatai, "Review of multilevel inverters for PV energy system applications," *Energies*, vol. 14, no. 6, pp. 1–23, 2021. [CrossRef]
5. S. Kouro, J. I. Leon, D. Vinnikov, and L. G. Franquelo, "Grid-connected photovoltaic systems: An overview of recent research and emerging PV converter technology," *IEEE Ind. Electron. Mag.*, vol. 9, no. 1, pp. 47–61, 2015. [CrossRef]
6. H. Nisar, A. Kashif Janjua, H. Hafeez, S. shakir, N. Shahzad, and A. Waqas, "Thermal and electrical performance of solar floating PV system compared to on-ground PV system-An experimental investigation," *Sol. Energy*, vol. 241, no. March, pp. 231–247, 2022. [CrossRef]
7. A. Gholami, M. Ameri, M. Zandi, and R. G. Ghoachani, "Electrical , thermal and optical modeling of photovoltaic systems : Step-by-step guide and comparative review study," *Sustain. Energy Technol. Assess.*, vol. 49, p. 101711, 2022. [CrossRef]
8. R. Passey, T. Spooner, I. Macgill, M. Watt, and K. Syngellakis, "The potential impacts of grid-connected distributed generation and how to address them : A review of technical and non-technical factors," *Energy Policy*, vol. 39, no. 10, pp. 6280–6290, 2011. [CrossRef]
9. P. Radatz, N. Kagan, C. Rocha, J. Smith, and R. C. Dugan, "Assessing maximum DG penetration levels in a real distribution feeder by using OpenDSS," *Proc Int Conf Harmon Qual Power, ICHQP*, vol. 2016, pp. 71–76, 2016. [CrossRef]
10. G. W. Chang, Y. H. Chen, L. Y. Hsu, Y. Y. Chen, Y. R. Chang, and Y. D. Lee, *Study of Impact on High PV-Penetrated Feeder Voltage Due to Moving Cloud Shadows*, 2016. [CrossRef]
11. D. T. Cotfas, P. A. Cotfas, and O. M. Machidon, "Study of temperature coefficients for parameters of photovoltaic cells,", *International Journal of Photoenergy*, vol. 2018, 1–12, 2018. [CrossRef]
12. S. Mohanty, S. Tripathy, S. R. Ghatak, and A. Mohapatra, *Impact Assessment of PV Penetration on Unbalanced Distribution Network with Dynamic Load Condition*, 2022, pp. 1–6. [CrossRef]
13. R. C. Dugan, and T. E. McDermott, "An open source platform for collaborating on smart grid research," *IEEE Power Energy Soc Gen. Meet*, pp. 1–7, 2011. [CrossRef]
14. W. H. Kersting, "Radial distribution test feeders," *IEEE Trans. Power Syst.*, vol. 6, no. 3, pp. 975–985, 1991. [CrossRef]
15. S. S. Ram, S. B. Daram, P. S. Venkataramu, and M. S. Nagaraj, "Analysis of ZIP load modeling in power transmission system," *Int. J. Control Autom.*, vol. 11, no. 7, pp. 11–24, 2018. [CrossRef]
16. A. J. Collin, "*Advanced load modelling for power system studies doctor of philosophy*," Univ. Edinburgh.
17. M. Diaz-Aguilo *et al.*, "Field-validated load model for the analysis of CVR in distribution secondary networks: Energy conservation," *IEEE Trans. Power Deliv.*, vol. 28, no. 4, pp. 2428–2436, 2013. [CrossRef]
18. EPRI, *OpenDSS PVSystem Element Model Version 1*, 2011, pp. 1–10.
19. T. Ehara, *IEA-PVPS Task10/ PVUPSCALE: Overcoming PV Grid Issues in the Urban Areas*, 2009, p. 82.
20. "CanmetENERGYLaboratory," *High-Resolution Solar Radiation Datasets*," nrcan.gc. Available: https://www.nrcan.gc.ca/energy/renewable-electricity/solar-photovoltaic/18409
21. T. Zhang, P. W. Stackhouse, W. S. Chandler, J. M. Hoell, D. Westberg, and C. H. Whitlock, "A global perspective on renewable energy resources: NASA's Prediction of Worldwide Energy Resources (POWER) Project," *ISES Sol. World Congr.*, vol. 4, 2007, pp. 2636–2640. [CrossRef]
22. E. Skoplaki, A. G. Boudouvis, and J. A. Palyvos, "A simple correlation for the operating temperature of photovoltaic modules of arbitrary mounting," *Sol. Energy Mater. Sol. Cells*, vol. 92, no. 11, pp. 1393–1402, 2008. [CrossRef]
23. C. Demoulias, "A new simple analytical method for calculating the optimum inverter size in grid-connected PV plants," *Electr. Power Syst. Res.*, vol. 80, no. 10, pp. 1197–1204, 2010. [CrossRef]
24. S. Emiroglu, Y. Uyaroglu, and G. Ozdemir, "Distributed reactive power control based conservation voltage reduction in active distribution systems," *Adv. Electr. Comp. Eng.*, vol. 17, no. 4, pp. 99–106, 2017. [CrossRef]